

# 3

## Satellite Orbits

### 3.1 Introduction

As discussed in Chapters 1 and 5, Interferometric synthetic aperture radar (InSAR) can measure surface deformation to a fraction of the radar wavelength of 10–20 mm. This involves two basic measurements that are equally important and should ideally have similar accuracy. The first is the range between the satellite and a reflector on the surface of the Earth, which is measured from the two-way travel time of the radar waves. The second is the position of the satellite with respect to an Earth-fixed coordinate system. The precise trajectory of the satellite is computed using GNSS and laser tracking systems combined with satellite orbit dynamic calculations (e.g., Teunissen and Montenbruck (2017)). This precise orbit is used in four areas of the InSAR processing discussed later in this chapter: proper focus of the SAR image; projection of the reference topography from geographic to radar coordinates (i.e., *back projection*); alignment of the reference and repeat SAR images; and flattening of the interferogram. These are the four main steps of traditional InSAR processing. A newer approach uses the orbit to directly focus the SAR image onto a reference Earth topography, which is known as *geocoded single look complex* (SLC) processing as discussed in Section 5.10. These approaches rely on precise orbits having accuracies of a few centimeters. This orbital information is provided with the SAR data as a *state vector*, which consists of the Cartesian position  $\mathbf{x}$  and velocity  $\mathbf{v}$  of the satellite as a function of time. The six-element state vectors are provided at regular intervals at sub-mm precision (Table 3.1). Later in this chapter we describe how the discrete state vectors are interpolated in time using a Hermite polynomial interpolator. This interpolation is at the core of any InSAR processing system.

Before diving into the largely opaque numerical orbit calculations, it is worth reviewing some basic orbit geometry and dynamics. As shown in Figure 3.1, there are two basic types of satellite orbits called *near polar* and *geostationary*.

Table 3.1 Example state vectors for the Sentinel-1 satellite (\***LED** in GMTSAR).

year	day	seconds	X (m)	Y (m)	Z(m)	Vx(m/s)	Vy(m/s)	Vz(m/s)
2015	145	6334.00	-3254984.5766	-5923132.6241	2088724.6473	-350.947452	2705.794737	7091.076582
2015	145	6344.00	-3258291.5669	-5895740.5804	2159516.0837	-310.428195	2772.553006	7067.077378
2015	145	6354.00	-3261192.7003	-5867682.7971	2230063.5333	-269.776909	2838.941373	7042.279672
2015	145	6364.00	-3263686.6821	-5838963.0117	2300359.0251	-228.998736	2904.952133	7016.686286
2015	145	6374.00	-3265772.2692	-5809585.0386	2370394.6167	-188.098844	2970.577632	6990.300137
2015	145	6384.00	-3267448.2704	-5779552.7686	2440162.3955	-147.082425	3035.810270	6963.124233
2015	145	6394.00	-3268713.5465	-5748870.1679	2509654.4793	-105.954694	3100.642499	6935.161670
2015	145	6404.00	-3269567.0106	-5717541.2783	2578863.0174	-64.720890	3165.066825	6906.415639
2015	145	6414.00	-3270007.6282	-5685570.2159	2647780.1916	-23.386274	3229.075810	6876.889419
2015	145	6424.00	-3270034.4175	-5652961.1712	2716398.2166	18.043873	3292.662073	6846.586380
2015	145	6434.00	-3269646.4498	-5619718.4079	2784709.3415	59.564247	3355.818288	6815.509981
2015	145	6444.00	-3268842.8494	-5585846.2631	2852705.8503	101.169526	3418.537188	6783.663770

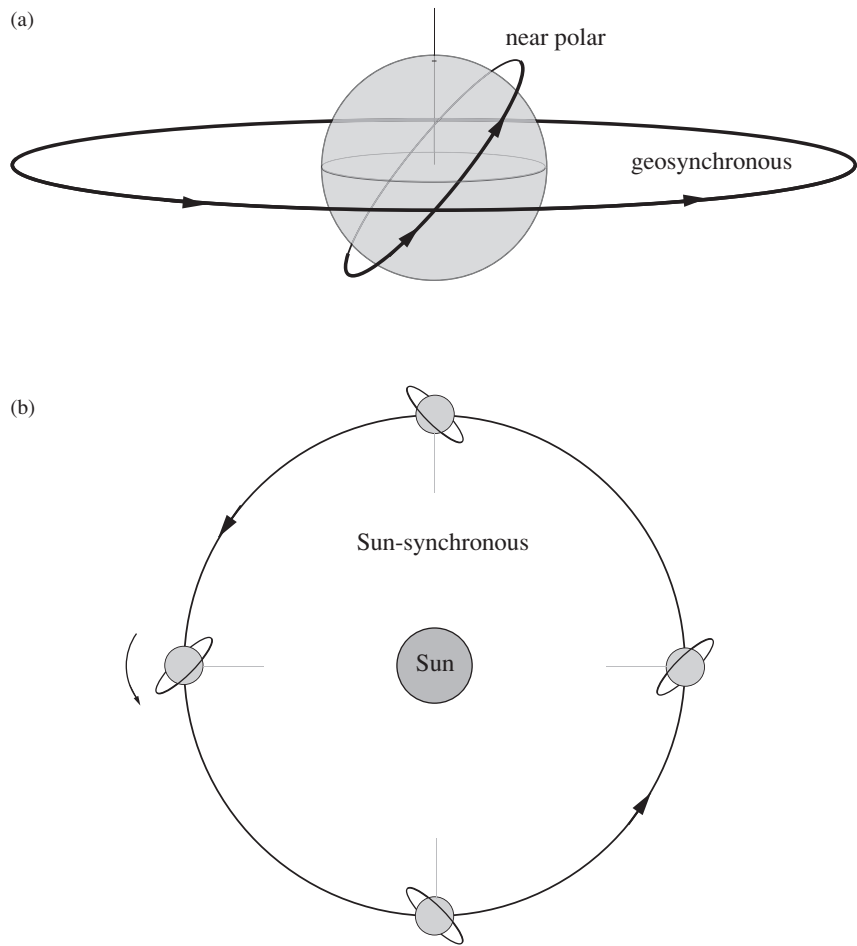


Figure 3.1 (a) The two most common types of orbits used for satellite remote sensing (near polar) and communications (geosynchronous). (b) A Sun-synchronous orbit has a precession rate of 1 year to maintain constant Sun illumination for optical sensors.

Near-polar orbits are commonly used for remote sensing applications. They have altitudes of between 400 and 1 500 km above the surface of the Earth. The orbit plane is inclined with respect to the equatorial plane of the Earth to achieve near-polar coverage. As discussed in the simple force balance calculation later, these satellites complete one orbit in about 6 000 seconds so their ground-track speed is about 6.7 km/s. The equatorial bulge of the Earth causes the orbit plane to precess like a top. The rate of precession can be adjusted to achieve a particular orbit repeat cycle or maintain a constant Sun illumination. The *Sun-synchronous orbit* (discussed later) is used by optical remote sensing satellites to maintain a constant Sun illumination direction. Satellites in geosynchronous orbit have an orbital period of one *sidereal day* (86 164 s), which requires a much larger orbital radius of 42 000 km. These satellites remain fixed at a particular longitude above the Earth's equator and are used mainly for communications as well as to track large-scale weather patterns. InSAR satellites are usually placed at low altitudes of  $\sim 700$  km and have high inclinations for near full Earth coverage.

### 3.2 Kepler Elements

As discussed earlier, the trajectory of a satellite can be most accurately described by a time series of state vectors having three position elements and three velocity elements. A second way of describing the satellite orbit is through six Kepler elements (Kaula, 1966). The geometry of a satellite in an elliptical orbit around the Earth is shown in Figure 3.2.

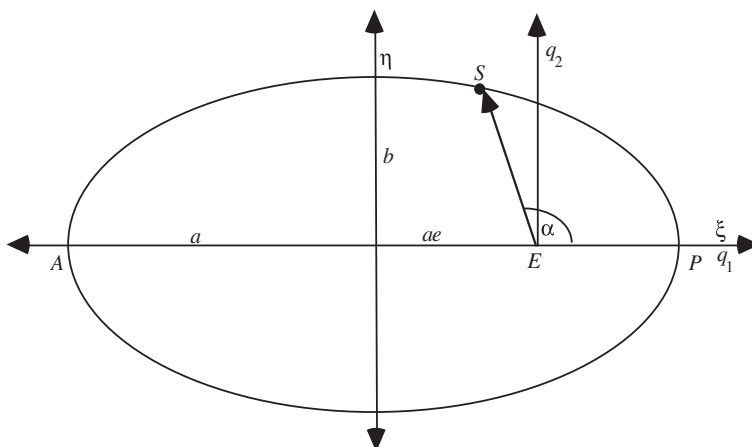


Figure 3.2 Diagram of a satellite  $S$  in an elliptical orbit around the Earth  $E$ .

The important parameters of the elliptical orbit are:

$S$  – satellite

$E$  – Earth

$A$  – apogee

$P$  – perigee

$\alpha$  – true anomaly (instantaneous angle from satellite to perigee)

$a$  – semimajor axis

$b$  – semiminor axis

$e$  – eccentricity

where  $e^2 = \frac{a^2 - b^2}{a^2}$ .

Note they are not all independent, so, for example, the semiminor axis can be replaced by the eccentricity parameter. Three of these parameters,  $\alpha$ ,  $a$ , and  $e$ , are Kepler elements describing the size and shape of the orbit.

Kaula (1966) solves the general force balance for a particle of negligible mass in orbit about a large point mass  $M$ . He shows that the orbit follows an ellipse where the angular momentum  $r^2 \frac{d\alpha}{dt}$  remains constant. This is Kepler's second law. The shape of the ellipse and the orbital radius versus the true anomaly are

$$\frac{\xi^2}{a^2} + \frac{\eta^2}{b^2} = 1 \Rightarrow r(\alpha) = \frac{a(1 - e^2)}{1 + e \cos \alpha}. \quad (3.1)$$

For an elliptical orbit about a point mass, the orbit frequency is given by

$$\omega_s = \left( \frac{GM}{a^3} \right)^{1/2}, \quad (3.2)$$

and the period of the orbit is  $T_s = \frac{2\pi}{\omega_s}$  where  $GM$  ( $3.98... \times 10^{14} \text{m}^3 \text{s}^{-2}$ ), the gravitational constant times the mass of the Earth, is one of the most accurately determined constants in Earth science. We can check this result for the simple case of a circular orbit. Consider a force balance on a small mass  $m$  orbiting the Earth (Figure 3.3).

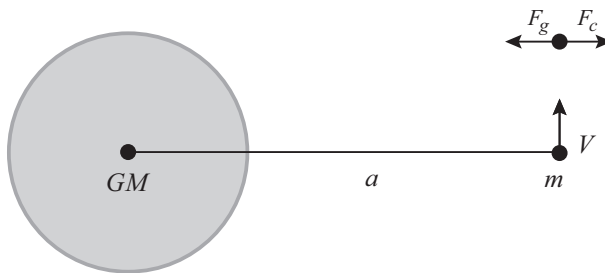


Figure 3.3 Force balance diagram of a small satellite of mass  $m$  in orbit about the Earth with a much larger mass  $M$ .

The inward-directed force of gravity is  $F_g = m\frac{GM}{a^2}$ , while the outward-directed centrifugal force is  $F_c = m\frac{V^2}{a} = ma\omega_s^2$  where  $V$  is the velocity of the satellite.

Equating these forces, we find  $\omega_s = \left(\frac{GM}{a^3}\right)^{1/2}$ . Note that the orbital frequency decreases with increasing orbit radius  $a$ . A typical polar-orbiting satellite has an altitude of 700 km so an orbital radius of 7 071 km and an orbit period of 5 921 s. The circumference of the Earth is about 40 000 km so the ground track speed of this satellite is 6.75 km/s. A satellite in a higher orbit of 1 500 km has a ground track speed of 5.8 km/s. As discussed in Chapter 2, this nominal velocity of  $\sim 6$  km/s places a lower bound on the pulse repetition frequency of  $2V/L$  or 1 200 Hz for a 10 m long antenna.

A geosynchronous satellite orbits the Earth in one sidereal day (86 164 s – the rotation period in an inertial frame) so must have an orbital radius of 42 000 km.

Figure 3.4 shows the elliptical satellite orbit placed in an Earth-centered, quasi-inertial coordinate system where the  $z$ -axis points toward the north pole, the  $x$ -axis points toward the Sun, and the  $y$ -axis is  $90^\circ$  east along the equatorial plane of the Earth. The orientation of the elliptical orbit plane in this system is defined by three angles, which are three additional Kepler elements. They are the inclination of the orbit plane with respect to the equatorial plane of the Earth ( $i$  – inclination), the longitude of the point where the ascending orbit crosses the equatorial plane of the Earth ( $\Omega$  – longitude of node), and the angle between the ascending crossing point (node) and perigee ( $\omega$  – argument of perigee). In summary, a complete description of an ideal elliptical orbit is described by six Kepler elements:

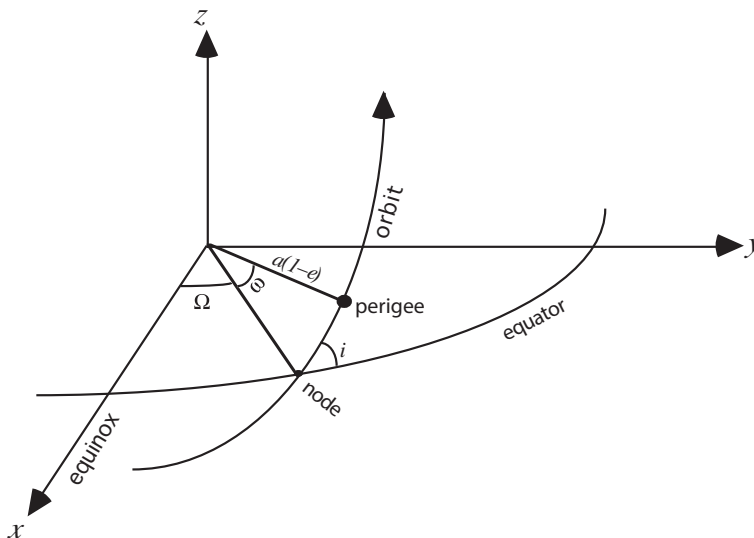


Figure 3.4 Diagram of the elliptical orbit in a quasi-inertial coordinate system.

$\alpha$  – true anomaly (instantaneous angle from satellite to perigee)

$\omega$  – argument of perigee

$\Omega$  – longitude of node

$a$  – semimajor axis

$e$  – eccentricity

$i$  – inclination.

### 3.3 Precession of the Orbit Plane

Because the Earth rotates, it is not spherical and is better described by an oblate ellipse (spheroid). A more precise description of the Earth's gravity potential field is

$$V(r, \theta) = \frac{-GM}{r} \left[ 1 - J_2 \frac{a_e^2}{2r^2} (3\sin^2\theta - 1) \right], \quad (3.3)$$

where:

$\theta$  – latitude

$a_e$  – equatorial radius

$J_2$  – dynamic form factor =  $1.08 \times 10^{-3}$ .

The dynamic form factor reflects the extra mass on the equatorial bulge of the Earth. The gravitational attraction of an oblate spheroid has two effects on the orbit. First, it decreases the orbit frequency (increases the period). Second, it causes the orbit plane to precess with respect to the inertial frame. The precession occurs because the equatorial bulge of the gravity field exerts a torque on the angular momentum vector of the orbit plane (Figure 3.5).

For a circular orbit, the precession frequency is given by

$$\frac{\omega_n}{\omega_s} = -\frac{3J_2}{2} \left( \frac{a_e}{a} \right)^2 \cos i = \frac{T_s}{T_n}, \quad (3.4)$$

where:

$\omega_n = \frac{2\pi}{T_n}$  – precession frequency and period  $T_n$

$\omega_s = \frac{2\pi}{T_s}$  – satellite orbit frequency and orbit period

$a_e$  – equatorial radius

$a$  – orbital radius

$J_2$  – dynamic form factor =  $1.08 \times 10^{-3}$

$i$  – inclination of satellite orbital plane.

Note the precession is retrograde for  $0 < i < 90^\circ$  and prograde for  $i > 90^\circ$ . Later we discuss how the orbit inclination and orbit radius can be adjusted so the precession is prograde and has a period of exactly 1 year.

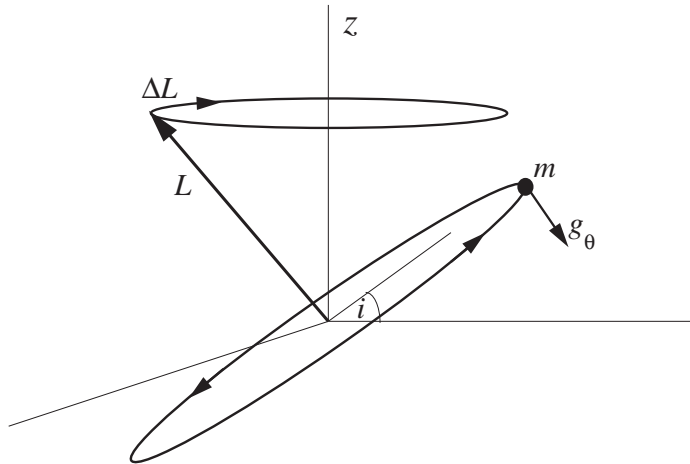


Figure 3.5 Satellite of mass  $m$  orbiting the Earth at an inclination  $i$ . The orbit has an angular momentum vector  $L$  perpendicular to the orbital plane. The  $\theta$  component of the gravity vector applies a torque to the orbit, causing a retrograde precession of the angular momentum vector and thus a precession of the orbital plane.

### 3.4 Ground Track of Circular Orbit

(These Sections 3.4 through 3.6.6 are optional reading.) In many remote sensing applications, we would like to predict the path traced by the subsatellite point along the surface of the Earth (Figure 3.6). This could be accomplished by running an orbit simulation program. However, in many cases one only needs to know the approximate location or velocity of the satellite. Two applications include:

- Suppose you know the basic orbit parameters (Kepler elements) of a LANDSAT-type satellite and you want to know how long it will take before the satellite is over your target area.
- You have satellite altimeter profiles and you know the longitudes of their equator crossings. Given an equator crossing, you would like to know if the track intersects a particular area; this can be used to design an efficient way to search profiles. A related application is to align altimeter profiles along tracks so they can be compared to look for ocean variability. A crude alignment can be done using Kepler elements. Here we derive simple analytic formulas for the ground track of a satellite in a circular orbit about a rotating Earth.

Many remote sensing satellites have nearly circular orbits ( $e < 0.01$ ), so we'll assume  $e = 0.0$ . Since the orbit is circular, the argument of perigee  $\omega$  is no longer relevant. The basic problem is to map the position (Figure 3.7) of a satellite track in a circular orbit (inertial frame) into an Earth-fixed coordinate system (Figure 3.8).

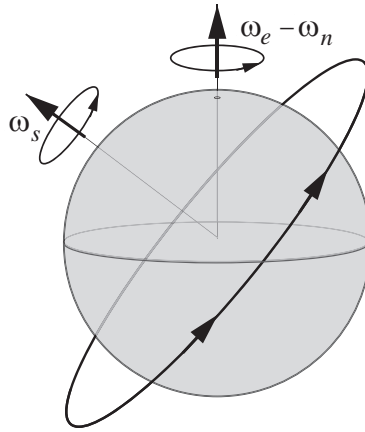


Figure 3.6 Satellite in a circular orbit around an elliptical Earth where:

$\omega_s$  – satellite orbit frequency

$\omega_e$  – Earth rotation frequency  $= 2\pi/86\,164$

$\omega_n$  – precession frequency.

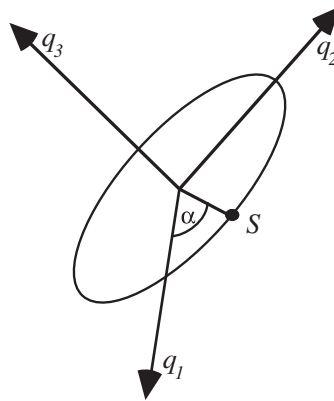


Figure 3.7 Satellite  $S$  in the coordinate system of the orbit plane where:

$q_1 = \cos \alpha = \cos \omega_s t$

$q_2 = \sin \alpha = \sin \omega_s t$

$q_3 = 0$ .

Let  $t = 0$  be the time when the satellite crosses the Earth's equator on an ascending orbit at a longitude of  $\lambda_0$ .

Two rotations are needed to align the satellite frame  $\mathbf{q}$  to the Earth-fixed frame  $\mathbf{x}$ . First, the  $\mathbf{q}$ -frame is rotated by an angle  $i$  about the  $q_1$  axis to account for the inclination of the orbit plane with respect to the Earth's equatorial plane. Second, the system is rotated about the  $x_3$  axis to account for the Earth's rotation rate minus the precession rate of the orbital plane in inertial space.



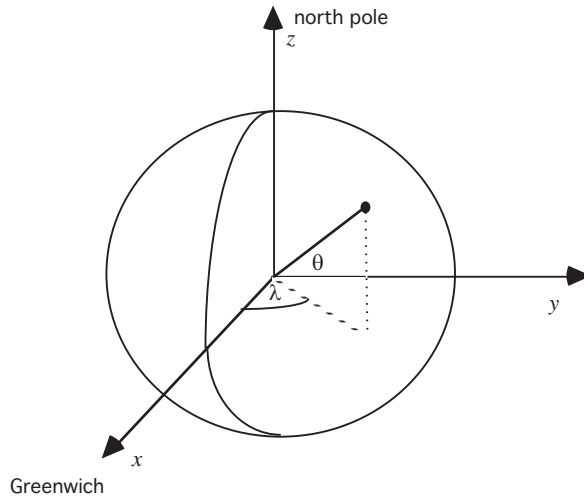


Figure 3.8 Earth-fixed coordinate system where:

$$\begin{aligned}x &= \cos \theta \cos \lambda \\y &= \cos \theta \sin \lambda \\z &= \sin \theta.\end{aligned}$$

Let  $\Omega = (\omega_e - \omega_n) t = \omega'_e t$  where  $\omega'_e$  is the Earth rotation rate minus the orbit precession rate. The satellite position in the **x**-frame is related to the satellite position on the **q**-frame as follows:

$$\mathbf{x} = \mathbf{R}_3(-\Omega) \mathbf{R}_1(i) \mathbf{q} \quad (3.5)$$

or

$$\begin{bmatrix} x \\ y \\ z \end{bmatrix} = \begin{bmatrix} \cos \Omega & \sin \Omega & 0 \\ -\sin \Omega & \cos \Omega & 0 \\ 0 & 0 & 1 \end{bmatrix} \begin{bmatrix} 1 & 0 & 0 \\ 0 & \cos i & -\sin i \\ 0 & \sin i & \cos i \end{bmatrix} \begin{bmatrix} \cos \alpha \\ \sin \alpha \\ 0 \end{bmatrix}. \quad (3.6)$$

By solving the rotations explicitly, one can derive analytical expressions for mapping from the satellite frame to the Earth-fixed frame and vice versa. Multiplying matrices yields

$$\begin{aligned}\cos \theta \cos \lambda &= \cos \Omega \cos \alpha + \sin \Omega \cos i \sin \alpha \\ \cos \theta \sin \lambda &= -\sin \Omega \cos \alpha + \cos \Omega \cos i \sin \alpha. \\ \sin \theta &= \sin i \sin \alpha\end{aligned} \quad (3.7)$$

The last equation relates latitude to the time since the equator crossing and vice versa.

$$\begin{aligned}\theta(t) &= \sin^{-1}(\sin \omega_s t \sin i) \\ t(\theta) &= \omega_s^{-1} \sin^{-1}\left(\frac{\sin \theta}{\sin i}\right)\end{aligned}\quad (3.8)$$

The cosine and sine of the longitude (relative to  $\lambda_o$ ) at some later time are given by

$$\begin{aligned}\cos \lambda &= \left( \frac{\cos \omega'_e t \cos \omega_s t + \sin \omega'_e t \sin \omega_s t \cos i}{\cos \theta} \right) \\ \sin \lambda &= \left( \frac{-\sin \omega'_e t \cos \omega_s t + \cos \omega'_e t \sin \omega_s t \cos i}{\cos \theta} \right).\end{aligned}\quad (3.9)$$

By combining these two expressions and adding the zero-time longitude, the longitude at a later time is

$$\lambda(t) = \tan^{-1} \left( \frac{-\sin \omega'_e t \cos \omega_s t + \cos \omega'_e t \sin \omega_s t \cos i}{\cos \omega'_e t \cos \omega_s t + \sin \omega'_e t \sin \omega_s t \cos i} \right) + \lambda_o. \quad (3.10)$$

These equations, 3.8 and 3.10, are approximate formulas to construct the ground track of a satellite in a circular orbit around a rotating Earth and we use them later to provide simple descriptions of the main types of satellite orbits.

### 3.5 Ellipsoidal Earth Model

Throughout this derivation we used *geocentric latitude*  $\theta$ , which is the angle between the equator and a line from the center of the Earth to the point on the surface of the Earth (Figure 3.9). However, *geographic latitude*  $\theta_g$  is more commonly used for Earth location and maps. Before satellites were available for geodetic work, one would establish latitude by measuring the angle between a local plumb line and an external reference point such as Polaris. Since the local plumb line is perpendicular to the local flattened surface of the Earth (i.e., *spheroid*), it points to one of the foci of the best-fitting elliptical model for the shape of the Earth.

The conversion between geocentric and geographic latitude depends on the flattening of the Earth  $f$  as shown in Figure 3.9.

The radius of the Earth versus latitude is

$$r(\theta) = \left( \frac{\cos^2 \theta}{a_e^2} + \frac{\sin^2 \theta}{c^2} \right)^{-1/2}, \quad (3.11)$$

where:

$a_e$  – equatorial radius = 6 378 135 m

$c$  – polar radius = 6 356 775 m (not to be confused with the speed of light in other chapters) and the flattening of the Earth is  $f = \frac{a_e - c}{a_e} \cong \frac{1}{298}$ .

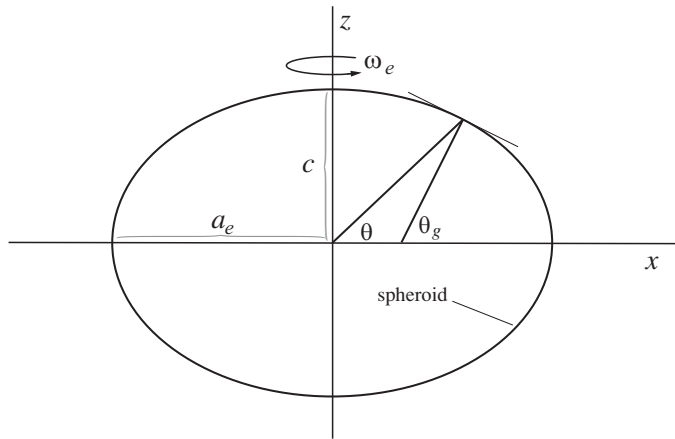


Figure 3.9 Approximate ellipsoidal shape of the Earth used to relate the geocentric and geographic latitudes.

The conversion between geocentric and geographic latitude is straightforward and is left as an exercise. The formulas are

$$\begin{aligned}\tan \theta &= \frac{c^2}{a_e^2} \tan \theta_g \\ \tan \theta &= (1 - f)^2 \tan \theta_g.\end{aligned}\tag{3.12}$$

To derive this equation, one starts with the equation for an ellipse  $\frac{x^2}{a_e^2} + \frac{y^2}{c^2} = 1$ . Then take the gradient of this equation and rearrange terms.

Example: What is the geocentric latitude at a geographic latitude of 45? The answer is 44.8, which amounts to a 22 km difference in location!

Later in the book we will need to convert a point from geodetic coordinates  $(\theta_g, \lambda, t)$ , where  $\lambda$  is longitude and  $t$  is topography above the reference ellipsoid, into Earth-fixed Cartesian coordinates  $(x, y, z)$  (Figure 3.8). The conversion is

$$\begin{aligned}x &= (N + t) \cos \theta_g \cos \lambda \\ y &= (N + t) \cos \theta_g \sin \lambda \\ z &= \left( \frac{c^2}{a_e^2} N + t \right) \sin \theta_g\end{aligned}\tag{3.13}$$

where

$$N = \frac{a_e^2}{\left( a_e^2 \cos^2 \theta_g + c^2 \sin^2 \theta_g \right)^{1/2}}.\tag{3.14}$$

### 3.6 Special Orbits

This simple circular orbit calculation provided the mathematical tools to describe several commonly used orbits.

$$\begin{aligned}\theta(t) &= \sin^{-1}(\sin \omega_s t \sin i) \\ t(\theta) &= \omega_s^{-1} \sin^{-1}\left(\frac{\sin \theta}{\sin i}\right)\end{aligned}\quad (3.15)$$

$$\lambda(t) = \tan^{-1}\left(\frac{-\sin \omega'_e t \cos \omega_s t + \cos \omega'_e t \sin \omega_s t \cos i}{\cos \omega'_e t \cos \omega_s t + \sin \omega'_e t \sin \omega_s t \cos i}\right) + \lambda_o, \quad (3.16)$$

#### 3.6.1 Zero Inclination Orbit

In this case,  $i = 0$ , and the orbit precession frequency is zero.

Using formulas for the sine and cosine of sums of angles (e.g.,  $\sin(a - b) = \sin a \cos b - \cos a \sin b$ ), one can simplify the longitude function to the obvious result

$$\lambda(t) = \tan^{-1}\left[\frac{\sin(\omega_s - \omega_e)t}{\cos(\omega_s - \omega_e)t}\right] = (\omega_s - \omega_e)t. \quad (3.17)$$

#### 3.6.2 Geostationary Orbit

In this case,  $i = 0$ ,  $\omega_s = \omega_e = 2\pi/86\,164$ .

The satellite orbit frequency matches the Earth rotation rate. From the Equation 3.2, we have an expression for the orbit frequency versus orbital radius. Geostationary required an orbital radius of 42 170 km or about 6.6 times the Earth radius. Usually this type of orbit is used for communications or for monitoring the weather patterns from a global perspective. Coverage of this type of orbit is a small circle of radius  $55^\circ$  centered on the subsatellite point. About six satellites are needed to provide a complete equatorial view of the Earth and these orbits are not used for high-latitude coverage.

#### 3.6.3 Geosynchronous Orbit

In this case,  $i \neq 0$ ,  $\omega_s = \omega_e$ .

With a nonzero inclination, this orbit can cover higher latitudes, but it spends only 1/2 of its time in the correct hemisphere. Inserting these parameters into the above-ground track equations and neglecting the precession frequency of the orbit plane, one obtains

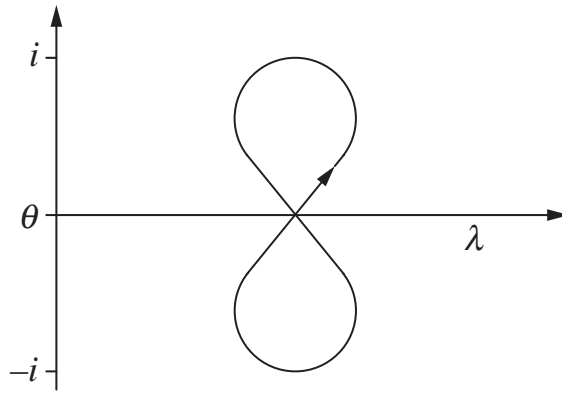


Figure 3.10 Ground track of a satellite in geosynchronous orbit traces out a figure 8.

$$\begin{aligned}\theta(t) &= \sin^{-1}(\sin \omega_e t \sin i) \\ \lambda(t) &= \tan^{-1} \left[ \frac{\cos \omega_e t \sin \omega_e t (\cos i - 1)}{\cos^2 \omega_e t + \cos i \sin^2 \omega_e t} \right].\end{aligned}\quad (3.18)$$

Now consider the case of small inclination, so  $\cos i \cong 1 - \frac{i^2}{2}$ . The denominator is about 1 and the numerator can be simplified, so the approximate results for longitude and latitude versus time are

$$\begin{aligned}\lambda(t) &= \tan^{-1} \left( \frac{i^2}{2} \frac{1}{2} \sin 2\omega_e t \right) \cong \frac{i^2}{4} \sin 2\omega_e t \\ \theta(t) &= \sin^{-1}(\sin \omega_e t \sin i) \cong i \sin \omega_e t.\end{aligned}\quad (3.19)$$

The latitude varies as a sine wave with a frequency of  $\omega_e$ , while the longitude varies like a sine wave with a frequency of  $2\omega_e$ . At  $t = 0$ , both the latitude and longitude are zero. The ground track of the orbit follows a figure 8 (Figure 3.10).

### 3.6.4 Sun-Synchronous Orbit

For many remote sensing applications, especially optical, it is important to have the ascending node pass over the equator at the same local time so the Sun illumination angle is the same on every orbit. To create a Sun-synchronous orbit, the plane of the orbit must precess in a prograde direction with a period of exactly 1 year.

$$\omega_n = 2\pi / (365.25 \times 86\,400) = 1.991 \times 10^{-7} \text{ s}^{-1}$$

Remember  $\frac{\omega_n}{\omega_s} = -\frac{3J_2}{2} \left( \frac{a_e}{a} \right)^2 \cos i$  so prograde precession requires  $i > 90^\circ$ . Thus the orbital inclination is dictated by the orbital altitude. For example, the

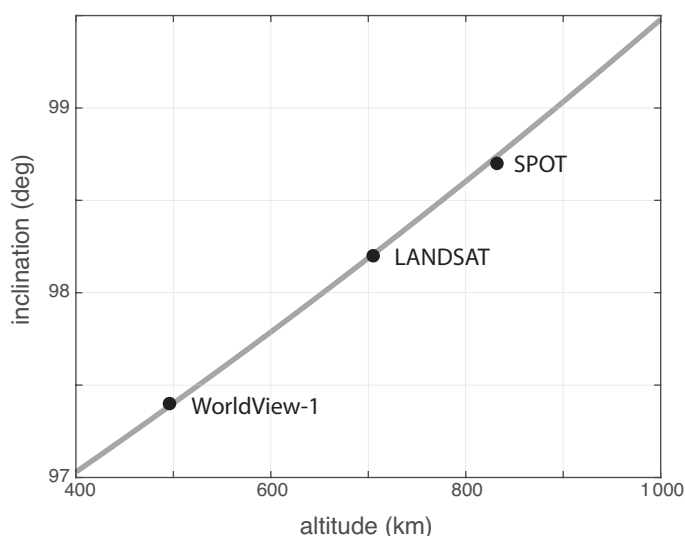


Figure 3.11 Inclination versus altitude for a Sun-synchronous orbit. Three examples of optical remote sensing satellites show excellent fits to this simplified analysis.

Sun-synchronous LANDSAT satellite has an orbital altitude of 705 km (radius  $a = 6\,980$  km) so must have an inclination of  $98.2^\circ$  (Figure 3.11). For a typical altitude range of remote sensing satellites of 400–1 000 km, the inclination for a Sun-synchronous orbit is quite narrow ( $97$ – $99.5^\circ$ ).

### 3.6.5 Orbits Tuned for Ocean Altimetry and InSAR

The following is desirable for ocean altimetry/InSAR:

- (a) Ascending and descending tracks should cross at a high angle to resolve both components of sea surface slope/deformation.
- (b) One should be aware of the aliasing of lunar and solar tides into the height/deformation.
- (c) One should choose a repeat cycle that will optimize spatial and temporal coverage.
- (d) High-latitude coverage may be desired for ice topography and deformation.

Example: The Geosat radar altimeter was launched in 1985 to measure the topography of the ocean surface in support of the Trident submarine program. The main objective of the first 1.5 years of the mission was to obtain complete marine coverage with tracks that cross at high angles for optimum gravity field recovery. An inclination of  $108^\circ$  provides the best compromise. However, this retrograde orbit

is nearly Sun-synchronous, which leads to aliasing of daily solar tide into a much longer period of time.

After Geosat completed its 1.5-year mapping mission, it began an extended repeat mission to observe changes in ocean topography associated with mesoscale currents. To measure changes, it was placed in an orbit having a ground track that repeats every 17.05 days. Of course, this was not optimal in terms of aliasing lunar and solar tides.

tide		period (hours)	period (days)	phase shift after 17.05 days
M2	principal lunar	12.421	0.5175	20°
K1	luni-solar	23.934	0.997	34°
S2	principal solar	12.00	0.500	36°
O1	diurnal lunar	25.819	1.076	54°

The Topex orbit was designed to minimize tidal aliasing. It was placed in a prograde orbit having an inclination of 66° and a repeat cycle of 10 days.

### 3.6.6 Exact Repeat Orbits

For applications measuring changes in surface deformation (i.e., InSAR) or changes in ocean topography (i.e., ocean altimetry), the orbit must retrace its ground track. To accomplish this there must be an integer relationship between the orbit frequency and the rotation rate of the Earth relative to the precessing orbit plane.

$$\frac{2\pi}{\omega_e - \omega_n} n_1 = \text{time for } n_1 \text{ rotations of the Earth relative to the orbit plane}$$

$$\frac{2\pi}{\omega_s} n_2 = \text{time it takes the satellite to complete } n_2 \text{ orbits}$$

Setting these two times to be equal provides an expression relating orbit frequencies to integer repeats.

$$\frac{2\pi}{\omega_e - \omega_n} n_1 = \frac{2\pi}{\omega_s} n_2 \Rightarrow \frac{\omega_e - \omega_n}{\omega_s} = \frac{n_1}{n_2}, \quad (3.20)$$

For example, consider the Sentinel-1 SAR, which has 175 orbit cycles in 12 days. This requires the following orbit frequencies:

$$\omega_e = 7.292 \times 10^{-5} \text{ s}^{-1}$$

$$\omega_s = 1.041 \times 10^{-3} \text{ s}^{-1}$$

$$\omega_n = \omega_e - \omega_s \frac{n_1}{n_2}.$$

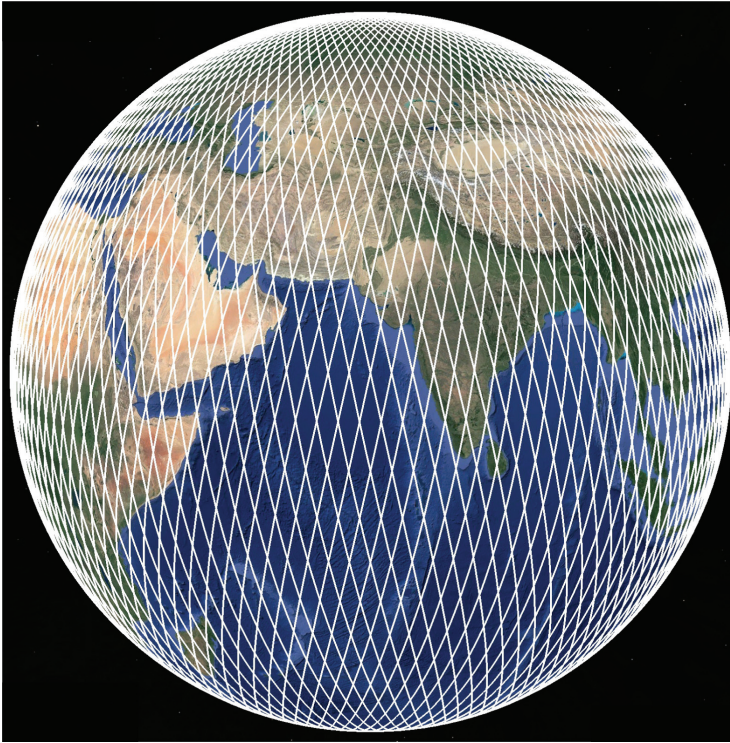


Figure 3.12 Ground track of Sentinel-1 computed using Equations 3.15 and 3.16 and an inclination of  $98.2^\circ$ .

An example of the Sentinel-1 ground track is shown in Figure 3.12. This is a retrograde orbit, so the ascending tracks go in a northwest direction and reach a maximum latitude of  $81.8^\circ$ .

### 3.7 Precise Orbits for InSAR

The earlier discussion on Kepler elements provides an overview of orbit kinematics and dynamics. However, these simple approaches are not sufficiently accurate for InSAR processing, which relies on orbit accuracy of 20–50 mm. In this section we describe the precise orbital information that is currently available with standard remote sensing products. The development of methods for constructing these precise orbits from a combination of precise tracking (GNSS, satellite laser ranging (SLR), and Doris) mainly comes from the radar altimeter community where they require radial orbit accuracy of better than 20 mm to achieve their objectives for monitoring global sea level (Cerri et al., 2010).

As shown in Table 3.1, the precise orbit is provided as state vectors having a time spacing of 10–60 seconds. The typical InSAR satellite travels 70 km during



the 10-second time interval, so there may be four or fewer state vectors during a typical 250 km SAR image frame. To perform the SAR processing, we will need a precise position every 1/2 antenna length or about every 5 m. Remarkably, mm-accuracy interpolation can be achieved by an algorithm called Hermite polynomial interpolation. For satellite orbits, the interpolator uses six position points and the corresponding six velocity points to construct a smooth interpolating function that exactly matches the six position and six derivative (velocity) points and provides a smooth interpolation between the central points. Note the state vectors need to extend at least three points before and after the frame for accurate interpolation. The state vectors provided with Radarsat-1 SAR data do not extend beyond the start and end of the SAR acquisition (frame), so the algorithm fails. The accuracy of the Sentinel-1 orbit is better than 30 mm in the radial and cross-track directions and 50 mm in the along-track direction. This precise orbital information is used in four aspects of the InSAR processing discussed next and is the key to robust and efficient software.

### 3.7.1 Proper Focus

First proper focus of the SAR image involves the coherent summation of range-aligned echoes over the length of the synthetic aperture as shown in Figure 3.13. This is discussed more completely in Chapter 4.

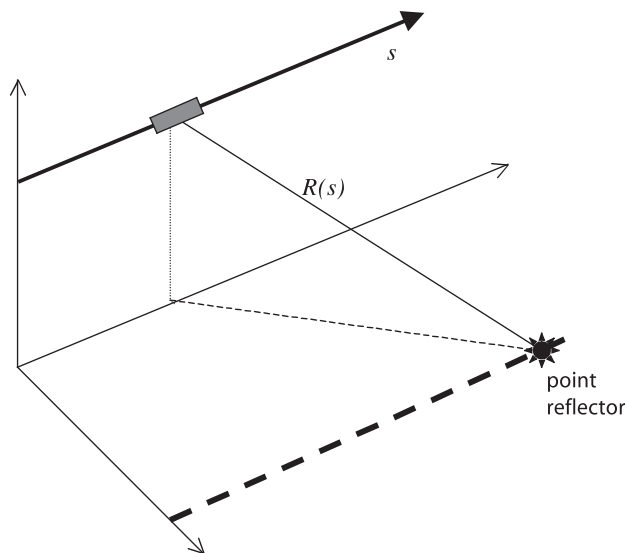


Figure 3.13 Geometry of SAR antenna flying over a point reflector on the ground. The range  $R$  varies with slow time  $s$  as measured by the precise orbit provided in an Earth-fixed coordinate system.

Therefore, we need to calculate the range as a function of slow time  $s$  (see definition of slow time in Figure 1.3.). First consider the case of a straight-line orbit passing over a fixed-point reflector. The range to the reflector would vary as a hyperbola with slow time. In the actual case, the orbital path is elliptical and the Earth is rotating so the range versus time function is a more complicated function. However, because the synthetic aperture is short ( $<5$  km) compared with the nominal range from the satellite to the reflector ( $\sim 800$  km), a three-parameter parabolic approximation is commonly used to model range versus time

$$R(s) = R_o + \dot{R}(s - s_o) + \frac{\ddot{R}}{2}(s - s_o)^2 + \dots \quad (3.21)$$

where  $R_o$  is the closest approach of the spacecraft to the point reflector and  $s_o$  is the time of closest approach. These three parameters,  $R_o$ ,  $\dot{R}$ , and  $\ddot{R}$ , are needed to focus an image (Chapter 4). In terms of the SAR processor, these are called the near-range  $R_o$ , the Doppler centroid  $f_{DC}$ , and the Doppler frequency rate  $f_R$ , which are related to the coefficients of this polynomial

$$f_{DC} = \frac{-2\dot{R}}{\lambda} \quad \text{and} \quad f_R = \frac{-2\ddot{R}}{\lambda}, \quad (3.22)$$

where  $\lambda$  is the wavelength of the radar. When a SAR image is focused at zero Doppler, the range rate at position  $s_o$  is by definition zero.

### 3.7.2 Transformation from Geographic to Radar Coordinates

The second use of precise orbital information is to map every point on the surface of the Earth (lon, lat, topography) into the range and azimuth coordinates of the radar. This back projecting (*SAT\_llt2rat* in GMTSAR) provides a lookup table (**trans.dat** in GMTSAR) for transforming between geographic and radar coordinates. The algorithm for creating this mapping is conceptually simple but can be computationally expensive. The precise orbital information is used to determine the range from the satellite to a topography grid cell. The approximate time of the minimum range is found using a golden section search algorithm (Press et al., 2007). A second-order polynomial is fit to this range versus time function about the time of minimum range (Equation 3.21). If the SAR image is focused at zero Doppler, then the range coordinate of the mapping is simply the minimum range and the azimuth coordinate is the time of the minimum range. Of course, by definition, the range rate (Doppler) is zero at this azimuth position. If the radar image was focused at a Doppler centroid other than zero, then Equation 3.22 can be used to calculate the nonzero range-rate at this Doppler.

$$\dot{R} = -\frac{\lambda f_{DC}}{2} \quad (3.23)$$

Next, by taking the derivative of the parabolic approximation, one can determine the along-track time shift that will be produced by focusing at a nonzero Doppler. This is given by

$$\Delta s = -\frac{\lambda f_{DC}}{2\ddot{R}}. \quad (3.24)$$

The corresponding range correction is given by

$$\Delta R = \frac{\ddot{R}}{2} \Delta s^2. \quad (3.25)$$

These two corrections are needed in the transformation from geographic to radar coordinates when the image is focused at a Doppler other than zero.

### 3.7.3 Image Alignment

The third use of the precise orbital information is to align the secondary images to the master image to sub-pixel accuracy in order to form the interferogram. (Note that *reference* and *repeat* images refer to individual interferograms, while *master* and *secondary* images refer to a geometrically aligned stack.) There are two main approaches to this image alignment.

The traditional alignment approach is done in three steps: (1) First, the orbital information is used to make a rough (1–2 pixel accuracy) estimate of the offset of the master and secondary images. (2) Then 2-D cross-correlation of sub-patches of data (e.g., 64 by 64 pixels) is used to estimate the affine transformations needed to map the secondary image onto the master image. As described earlier, the trajectories of the master and secondary images are very smooth so their differences in both the range  $dr$  and azimuth  $da$  coordinates are well described by the following equations:

$$\begin{aligned} dr &= c_0 + c_1 r_m + c_2 a_m \\ da &= c_3 + c_4 r_m + c_5 a_m, \end{aligned} \quad (3.26)$$

where  $r_m$  and  $a_m$  are the range and azimuth coordinates of the master image and there are six unknown coefficients  $c_0$  to  $c_5$ . The coefficients are determined by fitting planes to the range and azimuth offset data derived from the cross-correlation of the sub-patches. It seems reasonable that six parameters are sufficient to completely account for the affine transformation because the orbit is well described by a six-element state vector and the differences in the master and secondary state vectors are very small over the time span of the radar acquisition. (3) The final step is to use a 2-D sinc-function interpolator to resample the secondary image into the coordinates of the master image (*resamp* in GMTSAR). The accuracy of the alignment depends on the coherence between the master and secondary images. When coherence is high, the two images can be aligned to 0.1 pixel accuracy. When the

coherence is low, the alignment can be worse than 1.0 pixel. The method fails when the master and secondary images have poor correlation.

A second more accurate alignment approach utilizes the 50 mm accuracy of the precise orbits to perform the alignment geometrically. The advantage of this approach is that it is accurate to a small fraction of a pixel and there does not need to be any correlation between the master and secondary images. The preprocessing starts with a pixelwise estimate of range and azimuth offsets using precise orbits and a downsampled ( $\sim 360$  m) digital elevation model (DEM), which covers the region of the SLC satellite images. The precise orbit is used to back-project each pixel in the DEM (lon, lat, ellipsoidal height) into the range and azimuth coordinates of the master and secondary images. The algorithm first uses a golden section search method (Press et al., 2007) to quickly find the closest point at the PRF sampling between the orbital trajectory and the topography pixel. Then a polynomial refinement algorithm is used to improve the numerical accuracy to better than 10 mm in the azimuth coordinate. The range coordinate is the range between the antenna and the topography pixel evaluated at the corresponding azimuth coordinate. Note that the range rate or Doppler is zero at this closest point. A correction for alignment to a nonzero Doppler is discussed in Section 3.7.2. The differences between the range  $dr(r, a)$  and azimuth  $da(r, a)$  of the secondary image with respect to the master image are used to construct a dense look-up map of range and azimuth shifts, using a surfacing technique described in Smith and Wessel (1990). After these maps are generated, the coregistration is done pixelwise, which accounts for topography variation across the full image.

### 3.7.4 Flattening Interferogram

The fourth use of the precise orbit is for calculating the parallel and perpendicular components of the interferometric baseline that are needed for removing the interferometric phase for the range differences to every pixel in the image (*SAT\_baseline* in GMTSAR). This correction depends on both the orbital trajectory and the shape of the Earth, including the ellipsoidal, geoidal, and topographic components given in Chapter 4. If this is done in a consistent way, then long swaths of data can be calculated on a frame-by-frame basis and seamlessly merged in geographic coordinates. This is only possible because the baselines, orbital heights, and topographic data are all seamless at the frame boundaries. This seamless recombination of interferograms requires that the user select a common Earth radius and near range for the entire swath in the file *configure.txt* in GMTSAR. This feature is especially useful for ScanSAR-to-ScanSAR interferometry because each of the ScanSAR subswaths can be processed independently at their original azimuth sampling rate (i.e., PRF) and then reassembled in geographic coordinates without

adjustment. Frame-by-frame processing also has an advantage because the file size of one complex SAR image and its interferometric products can be far less than the 2 Gbyte file limit on older 32-bit computers. Second, one can easily take advantage of multiple processors that are available on many computers to process multiple frames of interferometric products simultaneously, without having to rewrite any computer code.

### 3.8 Problems

1. Precise orbital information is used in four areas of InSAR processing. Describe the four uses.
2. A satellite orbit can be represented by six parameters. Describe two approaches to defining these six parameters. How many parameters are needed to align a secondary image to a master image for interferometry? Why not more or fewer? (Also discussed in Section 8.5.)
3. The natural coordinates of a radar image have range or time along one axis and azimuth or slow time along the other axis. Why is the term slow time used?
4. Describe an algorithm to transform a point on the surface of the Earth (longitude, latitude, elevation) into radar coordinates.
5. When a SAR image is focused at zero Doppler, the radar coordinates of a point reflector correspond to the minimum range. Why? Derive the Equations 3.24 and 3.25 for adjusting the range and azimuth coordinates when an image is focussed at a nonzero Doppler.
6. GMTSAR uses a quadratic function to approximate the changes in baseline (horizontal and vertical) along the image frame. The quadratic formula is:

$$B(s) = a + bs + cs^2$$

where  $s$  is slow time ranging from the start to the end of the frame  $[0, T]$ . Suppose the actual baseline is measured at three times along the frame  $0, \frac{T}{2}, T$  and the values are  $B_1, B_2, B_3$ . Derive an expression for the parameters  $a, b, c$ . The forward model is

$$\begin{pmatrix} B_1 \\ B_2 \\ B_3 \end{pmatrix} = \begin{pmatrix} 1 & 0 & 0 \\ 1 & \frac{T}{2} & \frac{T^2}{4} \\ 1 & T & T^2 \end{pmatrix} \begin{pmatrix} a \\ b \\ c \end{pmatrix}.$$

7. Satellite orbital information is commonly provided as state vectors of position and velocity at regular intervals (e.g., 1 minute). Hermite polynomial interpolation is often used to interpolate the orbit to the full sampling rate of the radar (e.g., 2 000 Hz). What are the strengths and weaknesses of this approach? (This may require a literature search.)

8. Explain the terminology: master and secondary, reference and repeat.
9. Given a satellite in a circular orbit around the Earth at an orbital frequency of  $\omega_s$  and an inclination of  $i$ , develop a formula for the latitude velocity  $d\theta/dt$  of the satellite. (Assume a spherical Earth.) What happens when the inclination is  $90^\circ$ ? What happens when the inclination is  $0^\circ$ ?
10. Calculate the ground track for a satellite in a circular orbit about a spherical Earth. (Don't worry about converting from geocentric to geodetic coordinates.) Use this formula to calculate and plot the ground track of any remote sensing satellite. The following parameters will produce an exact 10-day repeat track for the Sentinel-1 satellite.

$$\omega_e = 2\pi/86\,164.1$$

$$\omega_s = 2\pi/5\,908$$

$$\omega_n = \omega_e - \omega_s \frac{12}{175}$$

$$i = 98.2 \frac{\pi}{180}$$

$$\theta(t) = \sin^{-1} [\sin \omega_s t \sin i]$$

$$t(\theta) = \omega_s^{-1} \sin^{-1} \left[ \frac{\sin \theta}{\sin i} \right]$$

$$\lambda(t) = \tan^{-1} \left[ \frac{-\sin \omega_e' t \cos \omega_s t + \cos \omega_e' t \sin \omega_s t \cos i}{\cos \omega_e' t \cos \omega_s t + \sin \omega_e' t \sin \omega_s t \cos i} \right] + \lambda_0$$